Reliable 3D mapping of ocular dominance columns in humans using GE-EPI fMRI at 7 T

Daniel Haenelt[1,2], Nikolaus Weiskopf[1], Roland Mueller[1], Shahin Nasr[3,4], Jonathan Polimeni[3,4], Roger Tootell[3,4], Martin Sereno[5], Robert Trampel[1]

[1]Department of Neurophysics, Max Planck Institute for Human Cognitive and Brain Sciences, Leipzig, Germany, [2]International Max Planck Research School on Neuroscience of Communication: Function, Structure, and Plasticity, Leipzig, Germany, [3]Athinoula A. Martinos Center for Biomedical Imaging, Massachusetts General Hospital, Charlestown, USA, [4]Department of Radiology, Harvard Medical School, Boston, USA, [5]Department of Psychology and Neuroimaging Center, San Diego State University, San Diego, USA

haenelt@cbs.mpg.de

Introduction

- At ultra-high magnetic fields ($\geq 7\,\mathrm{T}$), fMRI enables the delineation of mesoscale human functional structures.
- However, when using GE-EPI, the activation pattern may suffer from the well-known bias due to draining veins, especially close to the pial surface. [1]
- Measurement of functionally-based fine structures with known shape like ocular dominance columns (ODCs) in V1 [2] allows quantification of depth-dependent vascular blurring inherent to GE-EPI and other sequences.

Objectives

- Assessment of repeatability in measuring ODCs using GE-EPI.
- Direct visualization of hemodynamic blurring and column width estimation across cortical depth.

Methods

Experimental design

- One participant was invited for multiple scanning sessions on different days.
- ODCs were activated by alternating stimulation of single eyes using red/green moving random dots viewed through anaglyph goggles. [3]

MRI data acquisition

- 7 T whole-body MR scanner (MAGNETOM 7T, Siemens Healthineers, Erlangen, Germany).
- 32 channel phased array head coil (NOVA Medical Inc., Wilmington MA, USA).
- For functional data acquisition, 2D slices were acquired with either isotropic 0.8 mm (TR = 3 s, TE = 24 ms) or 1.0 mm (TR = 2 s, TE = 21 ms) nominal resolution, GRAPPA = 3 and pF = 6/8, covering early visual areas.

Analysis

- SPM12 was used for GLM analysis (no spatial smoothing).
- The cortex was segmented using FreeSurfer (cortical boundary surfaces were upsampled to 0.3 mm edge length).
- 10 surfaces at different cortical depths were created using the equi-volume approach. [4]
- Patches covering the stimulated area of V1 were manually defined and flattened.
- Flattened patches were interpolated onto a regular grid representation (isotropic 0.25 mm).
- Grids of single layers were stacked together to show functional contrasts across cortical depth.
- Autocorrelation maps and Fourier spectra were computed from the regular grid representation for column width estimation.

Results

1

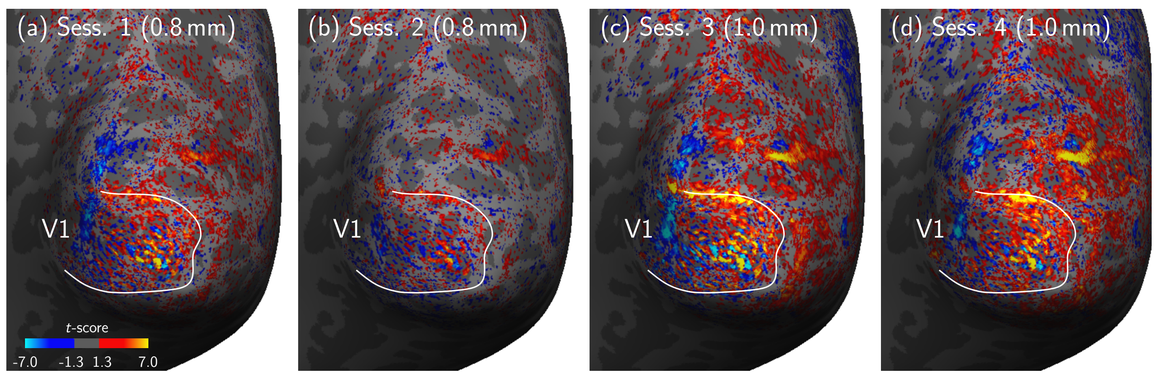

Activation maps Thresholded t-maps of ODCs (left eye > right eye) sampled from the central cortical layer of the right hemisphere. All sessions were acquired on different days. The white line demarcates the V1 border based on a separate retinotopy measurement [5]. The expected shape of ODCs within V1 can be reliably identified.

2

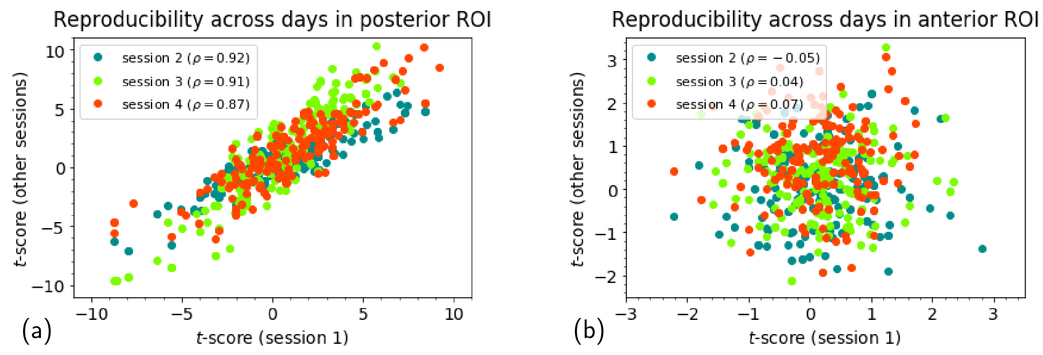

Reliability of ODC mapping Data points (t-scores; left > right; 1000 vertices) were sampled from the white matter surface of both hemispheres either (a) within (posterior ROI) or (b) directly outside (anterior ROI; control region) the stimulated area in V1. To account for spatial noise covariance, only randomly selected 10% of vertices were considered. Statistical significance of the Pearson correlation was assessed using a permutation analysis [3] and yielded a significance at the p = 0.001 level only for the posterior ROI.

3

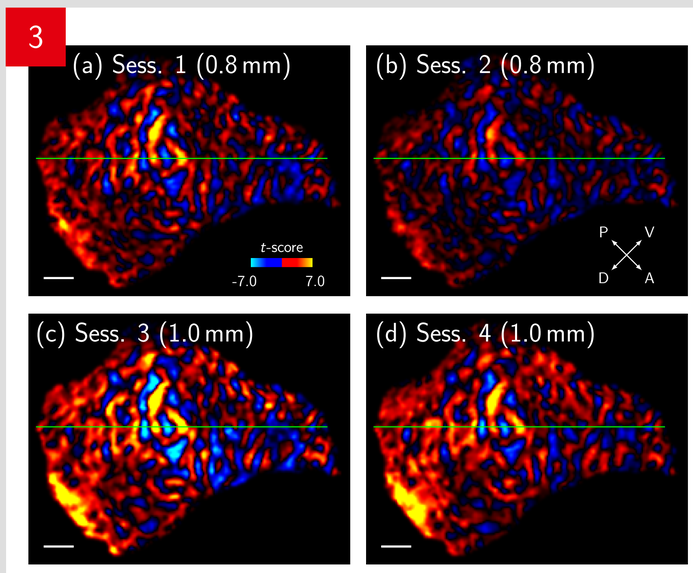

Regular grid representation Unthresholded t-maps (left > right) from the central cortical layer restricted to the stimulated region of V1. The green line shows the position of the cross-section shown in fig. 4. P: posterior, A: anterior, V: ventral, D: dorsal, white line: 5 mm.

4

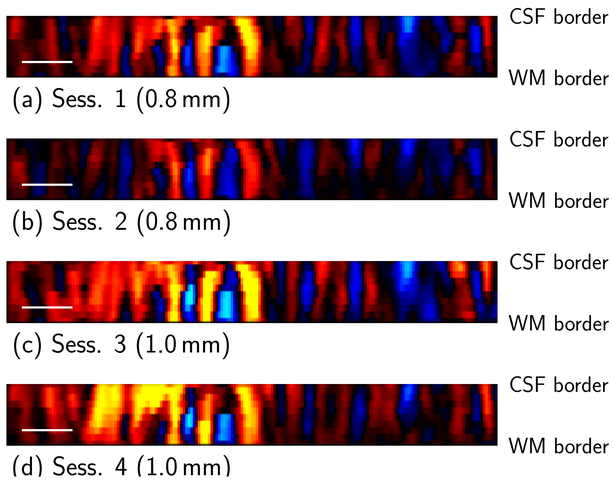

Cross-section of regular grid representation Unthresholded t-maps (left > right) at the position of the green line (fig. 3) through cortical depth. The blurring towards the pial surface can be identified in all profiles. Color-coding as in fig. 3. White line: 5 mm.

5

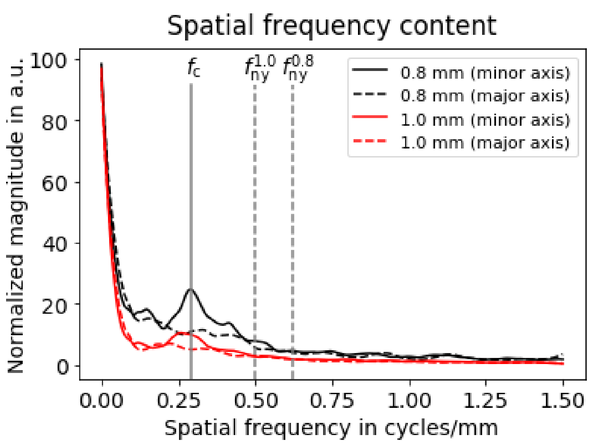

Spatial frequency distribution Fourier spectrum of unthresholded t-maps sampled from the central cortical layer (see fig. 3) and averaged over hemispheres and sessions with the same resolution in two orthogonal directions. Directions were defined as principal components of the Fourier spectrum [6]. A Savitzky-Golay filter was applied to single spectra. f_c: average cycle frequency of ODCs in minor axis direction. f_{ny}: Nyquist frequency.

6

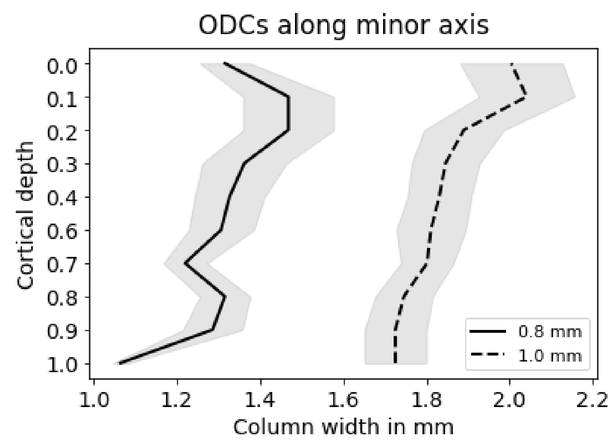

Column width The width of ODCs across cortical depth was estimated from the central peak (minor axis direction as described in fig. 5) FWHM of the autocorrelation map computed from unthresholded t-maps (left > right, see fig. 3). Width estimates were averaged across hemispheres and sessions with the same resolution. Increasing column width putatively caused by vascular blurring can be identified at both resolutions. However, estimates depend on voxel size. Shaded areas denote SEM.

Discussion

- The study demonstrates the feasibility of reliable ODC mapping across days using GE-EPI with isotropic 0.8 mm and 1.0 mm in line with [3].
- The regular grid representation of flattened cortical surfaces allows direct visualization of the hemodynamic blurring across cortical depth visible in all analyzed sessions.
- Column width estimation is biased by voxel size although ODCs can be reliably delineated at both resolutions.
- Future work will use this approach to study the cortical depth-dependent hemodynamic blurring inherent to different fMRI approaches (GE-BOLD, SE-BOLD, VASO).

References

[1] Polimeni J et al. *Neuroimage* 2010; 52:1334.
[2] Menon R et al. *J Neurophysiol* 1997; 77:2780.
[3] Nasr S et al. *J Neurosci* 2016; 36:1841.
[4] Wagstyl K Surface Tools *Github repository* 2018.
[5] Sereno M et al. *Science* 1995; 268:889.
[6] Borri M et al. *Med Phys* 2016; 43:6354.

OHBM, Rome, Italy, 2019, Poster number: W408